Low Endothelial Shear Stress Predicts Evolution to High-Risk Coronary Plaque Phenotype in the Future

A Serial Optical Coherence Tomography and Computational Fluid Dynamics Study

Erika Yamamoto, MD, PhD; Gerasimos Siasos, MD, PhD; Marina Zaromytidou, MD, PhD; Ahmet U. Coskun, PhD; Lei Xing, MD, PhD; Krzysztof Bryniarski, MD, PhD; Thomas Zanchin, MD; Tomoyo Sugiyama, MD, PhD; Hang Lee, PhD; Peter H. Stone, MD; Ik-Kyung Jang, MD, PhD

Background—Low endothelial shear stress (ESS) is associated with plaque progression and vulnerability. To date, changes in plaque phenotype over time in relation to ESS have not been studied in humans. The aim of this study was to investigate whether local ESS can predict subsequent changes to plaque phenotype using optical coherence tomography.

Methods and Results—A total of 25 coronary arteries from 20 patients who underwent baseline and 6-month follow-up optical coherence tomography were included. Arteries were divided into serial 3-mm segments, and plaque characteristics were evaluated in each segment. A total of 145 segments were divided into low-ESS group (ESS <1 Pa) and higher-ESS group (ESS ≥1 Pa) based on baseline computational flow dynamics analyses. At baseline, low-ESS segments had significantly thinner fibrous cap thickness compared with higher-ESS segments (128.2±12.3 versus 165.0±12.0 μm; *P*=0.03), although lipid arc was similar. At follow-up, fibrous cap thickness remained thin in low-ESS segments, whereas it significantly increased in higher-ESS segments (165.0±12.0 to 182.2±14.1 μm; *P*=0.04). Lipid arc widened only in plaques with low ESS (126.4±15.2° to 141.1±14.0°; *P*=0.01). After adjustment, baseline ESS was associated with fibrous cap thickness (β, 9.089; 95% confidence interval, 2.539–15.640; *P*=0.007) and lipid arc (β, −4.381; 95% confidence interval, −6.946 to −1.815; *P*=0.001) at follow-up.

Conclusions—Low ESS is significantly associated with baseline high-risk plaque phenotype and progression to higher-risk phenotype at 6 months.

Clinical Trial Registration—URL: http://www.clinicaltrials.gov. Unique identifier: NCT01110538.

(*Circ Cardiovasc Interv*. 2017;10:e005455. DOI: 10.1161/CIRCINTERVENTIONS.117.005455.)

Key Words: atherosclerosis ■ coronary vessels ■ shear stress ■ tomography, optical coherence

Endothelial shear stress (ESS), which is the biomechanical tangential force generated by the friction of blood flow on the endoluminal surface of an artery, heavily influences endothelial function and affects plaque development and progression. The proatherogenic effect of low ESS in subsequent plaque progression has been previously reported in animal and human studies.[1–9] In the PREDICTION study (Prediction of Progression of Coronary Artery Disease and Clinical Outcome Using Vascular Profiling of Shear Stress and Wall Morphology), Stone et al[10] showed the association between baseline ESS and plaque progression in humans with coronary artery disease using intravascular ultrasound. In addition, they demonstrated that low ESS and high plaque burden were independent predictors of future revascularization. Our group previously reported the association between local ESS and plaque characteristics in humans using optical coherence tomography (OCT) at a single time point.[11] Plaques with low ESS showed greater vulnerability compared with those with high ESS. The association between baseline ESS and subsequent changes of plaque characteristics and the influence of serial changes of ESS on plaque characteristics over time, however, has not been studied. Therefore, we assessed the influence of ESS on subsequent changes in microscopic plaque morphology in humans at baseline and follow-up using frequency-domain OCT.

Methods

Study Population

Study subjects were selected from the Massachusetts General Hospital OCT Registry, which is an international multicenter registry of

Received May 3, 2017; accepted June 28, 2017.

From the Cardiology Division, Massachusetts General Hospital (E.Y., L.X., K.B., T.Z., T.S., I.-K.J.), Biostatistics Center, Massachusetts General Hospital (H.L.), and Division of Cardiovascular Medicine, Brigham and Women's Hospital (G.S., M.Z., A.U.C., P.H.S.), Harvard Medical School, Boston, MA; and Division of Cardiology, Kyung Hee University Hospital, Seoul, Republic of Korea (I.-K.J.).

The Data Supplement is available at http://circinterventions.ahajournals.org/lookup/suppl/doi:10.1161/CIRCINTERVENTIONS.117.005455/-/DC1.

Correspondence to Ik-Kyung Jang, MD, PhD, Cardiology Division, Massachusetts General Hospital, Harvard Medical School, GRB 800, 55 Fruit St, Boston 02114, MA. E-mail ijang@mgh.harvard.edu

WHAT IS KNOWN

- Low endothelial shear stress is associated with a high-risk plaque phenotype.

WHAT THE STUDY ADDS

- Low endothelial shear stress is significantly associated with progression to higher-risk phenotype in 6 months, despite cholesterol-lowering therapy.

patients who have undergone OCT. The registry was approved by the institutional review board at each participating site. Written informed consent was obtained from all patients before enrollment. Inclusion criteria were (1) nonculprit lesions imaged by OCT at 2 time points, (2) frequency-domain OCT pullback length ≥20 mm between corresponding proximal and distal anatomic landmarks to be used for 3-dimensional (3D) reconstruction identified at both baseline and follow-up OCT studies, (3) ≥2 different angiographic projections of the examined coronary artery, (4) no history of previous stent implantation in the artery of interest, and (5) time interval from baseline to follow-up ≥3 months. Among 363 patients who had OCT images at both time points, 104 were excluded because they had only TD-OCT images, 195 because only the culprit lesion was imaged, 30 because of insufficient image length and suboptimal quality of OCT imaging for 3D reconstruction, 13 because of inability of matching images because of lack of anatomic landmarks, and 1 because of early follow-up <3 months. Finally, 20 patients (25 arteries) were included in the analysis.

Data Acquisition

A frequency-domain OCT system (St. Jude Medical, St. Paul, MN) was used in this study. The technique of intracoronary OCT imaging has been previously described.[12] All images were digitally stored, deidentified, relabeled, and submitted to Massachusetts General Hospital for analysis. After Z-offset calibration and lumen segmentation, OCT images were transferred as DICOM files (digital imaging and communications in medicine) to the Vascular Profiling Laboratory at Brigham and Women's Hospital for ESS computation.

Computational Fluid Dynamics and ESS Analysis

Vascular profiling used a methodology previously described and validated in vivo.[13,14] 3D coronary artery reconstruction was performed using coronary angiograms and frequency-domain OCT images. To locate the segments in this OCT investigation at 2 time points, 2 to 3 readily visible side branches were identified and used as reference markers for accurate comparison of the same segments over time. The 3D coronary reconstructions were further processed with computational fluid dynamics techniques to provide detailed characteristics of intracoronary blood flow and local ESS distribution. ESS at the lumen surface of the 3D reconstructed artery was calculated as the product of blood viscosity and the gradient of blood velocity at the wall. Detailed methods were described previously[11] and are provided in Methods in the Data Supplement.

Previous studies have shown 3-mm segments accurately reflect the local hemodynamic and vascular characteristics and are also appropriate for serial comparisons.[10] The entire reconstructed artery was divided into consecutive 3-mm segments starting at the inlet, and each 3-mm segment was characterized by a local predominant ESS value (defined as the minimum averaged ESS value over a 90° arc in each 3-mm segment). Previous studies have shown the proatherogenic role of local low ESS in human atherosclerosis in a similar demographic population using a threshold of 1.0 Pa.[10,11] Based on these studies, each segment was categorized as constituting a low-ESS group (baseline ESS <1 Pa) or a higher-ESS group (baseline ESS ≥1 Pa; Figure 1).

OCT Image Analysis

For serial comparison, regions at baseline were matched to those at follow-up using anatomic landmarks, such as side branches or calcium deposits. Cross-sectional OCT images were analyzed at every 1-mm interval for qualitative and quantitative parameters. Lipid-rich plaque was defined as plaque with lipid arc >90° in any cross-sectional image within the segment.[12,15,16] Fibrous cap thickness (FCT) of a lipid plaque was measured 3× at its thinnest part and averaged. Thin-cap fibroatheroma (TCFA) was defined as a lipid-rich plaque with FCT ≤65 μm.[15,17] A quantitative and qualitative assessment was performed using OCT offline analysis software (St. Jude Medical, St. Paul, MN) at the OCT Core Laboratory. All OCT images were analyzed by 2 independent investigators blinded to patient information. In the event of discordance between the readers, a consensus reading was obtained from a third independent investigator.

Statistical Analysis

Categorical variables are presented as counts (%), and continuous variables are expressed as mean±SE or median and interquartile range. For the comparison of the OCT parameters between low and higher ESS, as well as the baseline and follow-up within ESS subgroups, the generalized estimating equations approach was used to account for within-subject correlation because of the clustering of multiple segments within patients. The relationships between continuous baseline ESS and continuous outcome variables were also tested using generalized estimating equations approach. FCT and lipid arc values at follow-up were adjusted by corresponding values at baseline to account for any baseline differences. All tests were 2 tailed with an α level of 0.05. All statistical analyses were performed using SPSS 18.0 (SPSS, Inc, Chicago, IL).

Results

Baseline Characteristics

A total of 145 segments from 25 coronary arteries, which included 9 left anterior descending arteries, 8 left circumflex arteries, and 8 right coronary arteries, were analyzed. Baseline patient characteristics are shown in Table 1. The median interval from first to second OCT study was 205 (190–280) days. Half of the patients presented with an acute coronary syndrome, and a majority of patients were on statin treatment.

Baseline ESS and Follow-Up ESS

The median ESS value was 1.51 (1.08–2.09) Pa. Among 145 segments, 29 (20%) segments at baseline were classified as low ESS and 116 (80%) as higher ESS. In the majority (91.4%) of segments with higher ESS at baseline, ESS remained high at follow-up. Among the segments with low ESS at baseline, ESS remained low in half (48.3%) and became higher in the remainder (51.7%; Table 2).

ESS and Plaque Characteristics at Baseline

Table 3 shows the baseline and follow-up OCT parameters in each group. At baseline, the prevalence of lipid-rich plaque was not statistically different between segments with low and higher ESS (37.9% versus 23.3%; P=0.11). However, low-ESS segments had higher prevalence of TCFA (17.2% versus 3.4%; P=0.001) and thinner FCT (128.2±12.3 versus 165.0±12.0 μm; P=0.03). Lipid arc was not significantly different between these 2 groups (126.4±15.2° versus 131.7±5.6°; P=0.73).

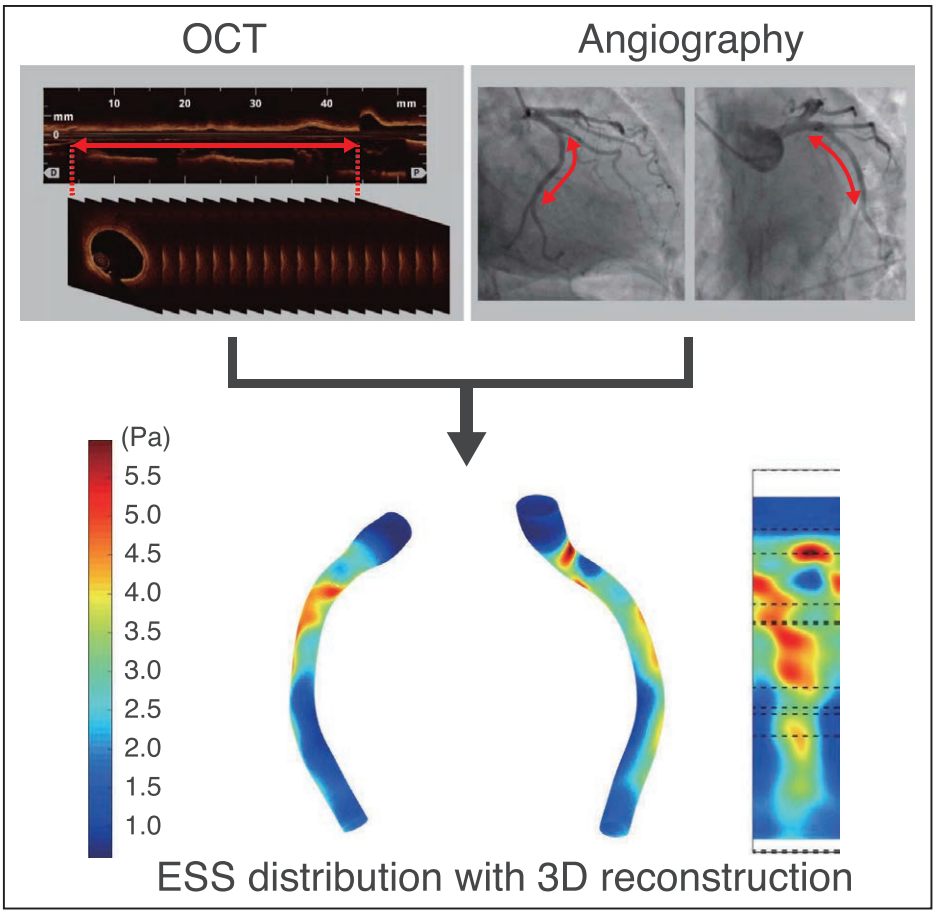

Figure 1. Representative image of 3D reconstruction with color-coded endothelial shear stress (ESS) values. Scale of ESS values is displayed on the vertical bar. OCT indicates optical coherence tomography.

Baseline ESS and Changes of Plaque Phenotype

In the overall population, FCT tended to increase (baseline, 154.3±9.6 μm versus follow-up, 166.8±11.3 μm; *P*=0.047), whereas lipid arc remained unchanged (baseline, 130.1±5.9° versus follow-up, 132.4±5.6°; *P*=0.59) during follow-up. Table 3 shows OCT parameters per segment at baseline and follow-up. The decrease of lumen area was significant only in segments with low ESS (baseline, 10.9±3.2 mm^2; follow-up, 10.4±3.1 mm^2; *P*=0.04). In segments with higher ESS at baseline, FCT significantly increased at follow-up (baseline, 165.0±12.0 μm versus follow-up, 182.2±14.1 μm; *P*=0.04), whereas it remained unchanged in segments with low ESS (128.2±12.3 versus 129.1±10.9 μm; *P*=0.90). Lipid arc significantly widened at follow-up only in segments with low ESS at baseline (baseline, 126.4±15.2° versus follow-up, 141.1±14.0°; *P*=0.01).

Although the changes of FCT from baseline to follow-up were not statistically different between the 2 groups (low ESS, 0.9±7.2 μm versus higher ESS, 17.2±7.2 μm; *P*=0.16), the changes in lipid arc were significantly different between the groups: lipid arc widened in segments with low ESS, whereas it became smaller in segments with higher ESS (low ESS, 14.7±6.3° versus higher ESS, −3.1±5.2°; *P*=0.02; Figure 2).

When OCT parameters were predicted by continuous measure of ESS, baseline ESS was predictive of both FCT (in a direct manner; β, 9.089; 95% confidence interval, 2.539–15.640; *P*=0.007) and lipid arc (in an inverse manner; β, −4.381; 95% confidence interval, −6.946 to −1.815; *P*=0.001) at follow-up after adjustment for baseline values (Table 4).

Longitudinal ESS and Plaque Characteristics

To evaluate the influence of ESS over time, segments with persistently low ESS (ESS <1 Pa both at baseline and at follow-up; N=14) were compared with other segments with higher ESS at least at one time point. The prevalence of lipid-rich plaque in segments with persistently low ESS was numerically higher, but not statistically different, than other segments at follow-up (42.9% versus 25.2%; *P*=0.15; Figure 3A). However, the prevalence of TCFA was significantly higher in segments with persistently low ESS than in others (14.3% versus 1.5%; *P*=0.007) at follow-up (Figure 3B). FCT was significantly thinner in segments with persistently low ESS compared with other segments at baseline (112.3±13.7 versus 164.4±10.6 μm; *P*=0.001) and did not significantly change at follow-up from baseline (baseline, 112.3±13.7 μm; follow-up, 117.5±11.4 μm; *P*=0.62), whereas among other segments with higher ESS for at least one time point, FCT significantly increased at follow-up from baseline, (baseline, 164.4±10.6 μm; follow-up, 178.6±12.7 μm; *P*=0.04). As a result, FCT at follow-up was significantly thinner in segments with persistently low ESS than in other segments (117.5±11.4 versus

Table 1. Patient Characteristics

	All Patients (N=20)
Clinical variables	
Age, y	58 (53–66)
Men	15 (75.0)
Hypertension	12 (60.0)
Diabetes mellitus	3 (15.0)
Dyslipidemia	14 (70.0)
Current smoker	6 (30.0)
Laboratory data	
Total cholesterol, mg/dL	193 (155–193)
LDL-cholesterol, mg/dL	112 (66–116)
HDL-cholesterol, mg/dL	39 (38–46)
Triglyceride, mg/dL	154 (83–168)
Creatinine, mg/dL	0.88 (0.77–0.98)
Medication	
ACE-I/ARB	5 (25.0)
Statin	18 (90.0)
Presentation	
STEMI	4 (20.0)
NSTE-ACS	6 (30.0)
Stable angina	10 (50.0)
Time from baseline to follow-up, d	205 (190–280)

Values are presented as N (%) or median (25th and 75th percentiles). ACE-I indicates angiotensin-converting enzyme inhibitor; ARB, angiotensin II reseptor blocker; HDL, high-density lipoprotein; LDL, low-density lipoprotein; NSTE-ACS, non-ST-segment elevation acute coronary syndrome; and STEMI, ST-segment–elevation myocardial infarction.

178.6±12.7 μm; $P<0.001$; Figure 3C). For lipid arc, there was no statistically significant difference between segments with persistently low ESS and other segments at follow-up (139.5±20.3° versus 130.5±4.8°; $P=0.63$; Figure 3D).

Segments with higher ESS were further classified into 2 groups: segments with persistently higher ESS (N=106) and segments with low ESS at one time point either at baseline or at follow-up (low→higher [N=15] and higher→low [N=10]). Segments that were exposed to low ESS at least at one time point had thinner FCT than those with persistently higher ESS (140.0±10.7 versus 190.8±15.4 μm; $P=0.01$; Figure 4).

Table 2. Association Between ESS at Baseline and ESS at Follow-Up

		Follow-Up		Total
		Higher (ESS ≥1.0 Pa)	Low (ESS <1.0 Pa)	
Baseline	Higher (ESS ≥1.0 Pa)	106 (91.4)	10 (8.6)	116
	Low (ESS <1.0 Pa)	15 (51.7)	14 (48.3)	29
	Total	121	24	145

Values are presented as N (%) of segments. ESS indicates endothelial shear stress.

Table 3. Qualitative and Quantitative Optical Coherence Tomography Parameters at Baseline and Follow-Up

Qualitative	Low ESS	Higher ESS	*P* Value*
Lipid-rich plaque			
Baseline	11 (37.9)	27 (23.3)	0.11
Follow-up	9 (31.0)	30 (25.9)	0.54
P Value†	0.10	0.36	
TCFA			
Baseline	5 (17.2)	4 (3.4)	0.001
Follow-up	3 (10.3)	1 (0.9)	0.03
P Value†	0.15	0.11	
Quantitative	**Low ESS**	**Higher ESS**	***P* Value***
Lumen area			
Baseline, mm^2	10.9±3.2	6.4±2.5	<0.001
Follow-up, mm^2	10.4±3.1	6.2±2.7	<0.001
P Value†	0.04	0.46	
FCT			
Baseline, μm	128.2±12.3	165.0±12.0	0.03
Follow-up, μm	129.1±10.9	182.2±14.1	0.003
P Value†	0.90	0.04	
Lipid arc			
Baseline, °	126.4±15.2	131.7±5.6	0.73
Follow-up, °	141.1±14.0	128.7±5.2	0.37
P Value†	0.01	0.54	

Values are presented as N (%) or median (25th and 75th percentiles). Low ESS, ESS at baseline <1.0 Pa and higher ESS, ESS at baseline ≥1.0 Pa. ESS indicates endothelial shear stress; FCT, fibrous cap thickness; and TCFA, thin-cap fibroatheroma.

*P value for low ESS vs higher ESS.

†P value for baseline vs follow-up.

Discussion

To the best of our knowledge, this is the first report that studied the association between local ESS and subsequent changes of plaque phenotype assessed by OCT in humans. The main findings of this study are (1) >90% of segments with higher ESS at baseline remained with higher ESS at follow-up, whereas about a half of segments with low ESS at baseline evolved to higher ESS at follow-up; (2) in segments with low ESS at baseline, FCT was thinner than in those with higher ESS at baseline and did not increase at follow-up. However, in segments with higher ESS at baseline, FCT was thicker at baseline and became even thicker at follow-up. Although baseline lipid arc was not significantly different between the 2 groups, only segments with low ESS exhibited significantly widened lipid arc at follow-up; (3) Baseline ESS, as a continuous variable, was directly associated with FCT and inversely associated with lipid arc at follow-up after adjustment for each baseline value; (4) In segments with persistently low ESS, prevalence of TCFA was significantly higher, and FCT was significantly thinner than other segments at follow-up.

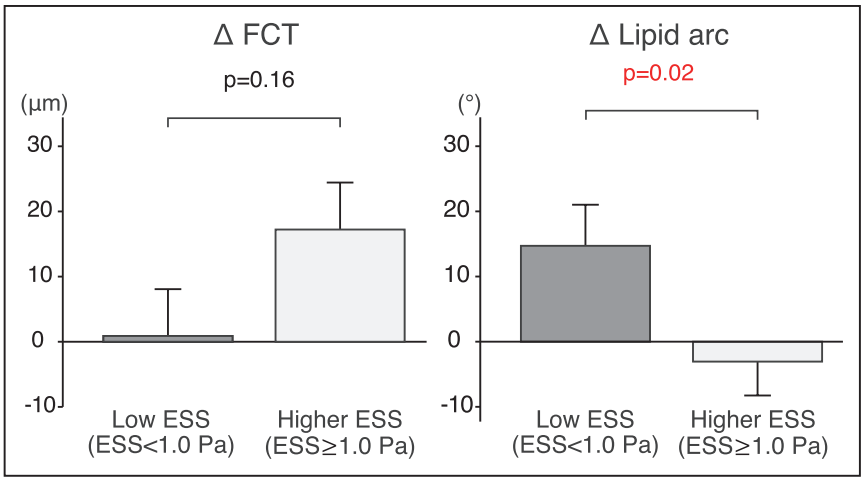

Figure 2. The change of fibrous cap thickness (FCT) and lipid arc. Although the change of FCT from baseline to follow-up was not different between the 2 groups, the change in lipid arc was significantly different between the groups. Error bars represent standard error of the mean. ESS indicates endothelial shear stress.

Dynamic Nature of ESS

In the current study, half of the segments with low ESS at baseline evolved to the higher ESS range at follow-up. This finding is consistent with a previous swine study, which demonstrated the dynamic nature of local ESS changes with 5 consecutive measurements.[2] Local ESS in lesions with low ESS frequently changed into higher ESS category at the next time point, likely related to changes in plaque progression and luminal obstruction or arterial remodeling. In our study, lumen area significantly decreased only in segments with low ESS, indicating that plaques with low ESS are prone to rapid progression of atherosclerosis resulting in higher ESS. This finding is consistent with the results of the PREDICTION study. We showed that segments with persistently low ESS had significantly thinner FCT than other segments. In addition, we found that segments that were exposed to low ESS at least at one time point either at baseline or at follow-up also had thinner FCT than those with persistently higher ESS. These results suggest a diagnostic value of ESS measurement at a single time point for future development of high-risk plaque.

Low ESS and Subsequent Plaque Progression, Transition to High-Risk Plaque Phenotype

Previous ex vivo and animal studies reported that lesions exposed to low ESS were associated with endothelial discontinuity, accumulation of inflammatory cells, increased expression of elastases and collagenases in the intima,[2,4] and migration and apoptosis of vascular smooth muscle cell,[18,19] leading to the thinning of FCT.[2,6] Low ESS has also been reported to be associated with inflammation[6] and lipid accumulation in the mouse carotid artery model,[7] as well as the swine coronary model.[1,6] Human studies using intravascular ultrasound have reported the association between local ESS and plaque progression.[8,10,20] Stone et al reported low ESS at baseline is an independent predictor of subsequent progression of plaque burden and luminal obstruction. However, intravascular ultrasound is limited by its insufficient resolution to visualize microscopic plaque architecture, such as TCFA, which has been reported to be responsible for two thirds of acute coronary syndromes.[21] Our group previously reported that TCFA was more frequent and FCT was thinner in lesions with low ESS.[11] However, our previous study only had a single time point for OCT imaging and ESS data. Therefore, the role of local ESS in longitudinal changes plaque vulnerability in humans was not previously known.

In the current study, we demonstrated the expansion of lipid arc at follow-up in plaques with low ESS at baseline. In this study, 90% of patients were on statin therapy with a significant reduction of low-density lipoprotein cholesterol level from 112 (66–116) mg/dL baseline to 77 (63–107) mg/dL at follow-up. In contrast, FCT became thicker at follow-up only in plaques with higher ESS. This finding indicates that the beneficial effect of statin on plaque stabilization is heterogeneous and mitigated in lesions with low ESS. This has potentially important clinical implications with respect to local preventive treatment of high-risk plaque with stenting.

ESS as Continuous Variables

ESS was associated with FCT and lipid arc at follow-up, when analyzed as a continuous variable. Previous animal studies have reported inflammatory cell infiltration and lipid deposition are closely and inversely associated with the magnitude of ESS.[6] This dose–response effect of ESS underscores that low ESS is likely one of the major underlying mechanisms for the heterogeneity of the coronary plaque within the same patient,

Table 4. Baseline ESS and Optical Coherence Tomography Parameters at Follow-Up (Continuous Variables)

Baseline Variables (Continuous)	Outcome (Continuous Various)	β (95% CI)	*P* Value
Baseline ESS (per 1 Pa increase)	Follow-up FCT, μm	9.089 (2.539–15.640)	0.007*
	Follow-up lipid arc, °	–4.381 (–6.946 to –1.815)	0.001†

CI indicates confidence interval; ESS, endothelial shear stress; and FCT, fibrous cap thickness.
*Adjusted baseline FCT.
†Adjusted baseline lipid arc.

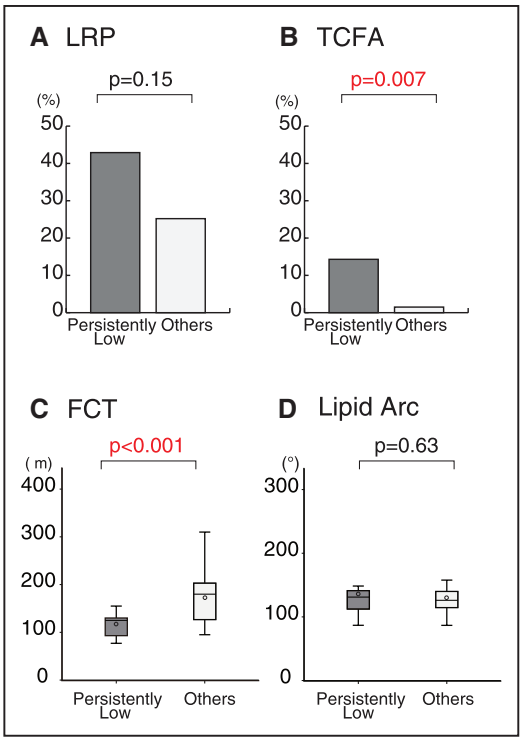

Figure 3. Optical coherence tomography parameters at follow-up in segments with persistently low endothelial shear stress (ESS) and others. The prevalence of lipid-rich plaque (LRP) in segments with persistently low ESS was numerically higher but not statistically different than other segments at follow-up (**A**). However, the prevalence of thin-cap fibroatheroma (TCFA) was significantly higher in segments with persistently low ESS than in other segments at follow-up (**B**). Although lipid arc was not significantly different between the 2 groups (**D**), fibrous cap thickness (FCT) at follow-up was significantly thinner in segments with persistently low ESS than in other segments (**C**). Black dots indicate mean value; persistently low, low ESS at baseline and follow-up; and others, higher ESS at least at one time point.

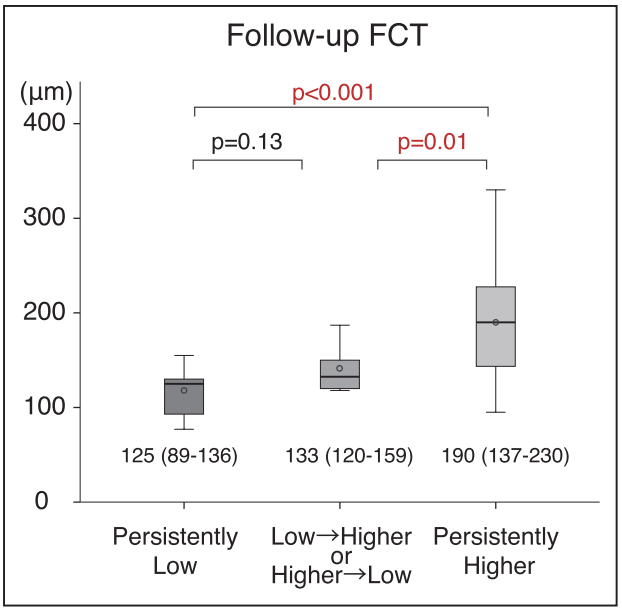

Figure 4. Follow-up fibrous cap thickness (FCT) and the changes of endothelial shear stress (ESS). Segments that were exposed to low ESS at least at one time point had thinner FCT than those with persistently higher ESS. Black dots indicate mean value; persistently low, low ESS at baseline and follow-up; low→higher, low ESS at baseline and higher ESS at follow-up; higher→low, higher ESS at baseline and low ESS at follow-up; and persistently higher, higher ESS at baseline and follow-up.

same vessel, and uneven distribution of plaque rupture in the coronary tree.[6]

Persistent Low-ESS Environment and High-Risk Plaque

Local ESS is dependent on anatomic configuration and geometric irregularities. The vascular response to plaque formation induces arterial remodeling and a change of geometry,[5] which subsequently results in changes of local ESS over time.[2]

Previous studies suggest that low ESS leads to plaque progression and excessive expansive remodeling, which in turn, lead to an ongoing low-ESS environment.[5,6] However, arterial remodeling responses are complex, particularly in atherosclerotic vessels in humans. Stone et al[9] reported both constrictive and expansive remodeling patterns in lesions exposed to low ESS. Another study reported low ESS was associated with constrictive remodeling,[8] which may reflect intraplaque hemorrhage within a high-risk plaque and a fibrotic, constrictive vascular response[22] or a physiological response within a normal artery segment to a low-ESS environment.[23] Factors other than local ESS are also involved in the determination of vascular responses. According to a natural history study, only 20% of plaques with initially low ESS develop excessive expansive remodeling and remain in a low-ESS environment.[24] In the current study, we analyzed the association between ESS at 2 time points and OCT parameters. Although the numbers were small, in the lesions with persistently low ESS at both baseline and follow-up, the prevalence of TCFA was significantly higher, and FCT was thinner at follow-up compared with other segments which were at least once exposed to high-ESS environment. This result demonstrates that persistent low ESS is a crucial factor for the development of high-risk plaques.

Limitations

First, the study was limited by a small sample size of patients. Despite the small sample size, we were able to clearly demonstrate the relationship between ESS and plaque phenotype. Second, we used OCT imaging only and not intravascular ultrasound, and, therefore, we were not able to assess the vascular remodeling pattern. Third, the presence of macrophage and superficial calcification may affect the detection of lipid components by OCT.[25] Fourth, because of small number of subjects, surrogate end points of plaque vulnerability were used instead of clinical outcome.

Conclusions

Low ESS is significantly associated with baseline high-risk plaque phenotype and progression to higher-risk phenotype within 6 months.

Acknowledgments

Dr Jang's research was supported by Mr Michael and Mrs Kathryn Park and by Mrs Gill and Mr Allan Gray. Dr Stone's laboratory was supported by the generosity of the Schaubert Family and the George Behrakis Research Foundation and St. Jude Medical Fellowship. We are grateful

to Michelle Cormier, BS (Senior Vascular Profiling Analyst, Vascular Profiling Laboratory, Brigham and Women's Hospital), for her extensive analytic input in the vascular profiling process.

Disclosures

Dr Jang has received grants and consulting fees from St. Jude Medical/Abbott, and Dr Stone has received a grant from St. Jude Medical/Abbott. The other authors report no conflicts.

References

1. Koskinas KC, Chatzizisis YS, Papafaklis MI, Coskun AU, Baker AB, Jarolim P, Antoniadis A, Edelman ER, Stone PH, Feldman CL. Synergistic effect of local endothelial shear stress and systemic hypercholesterolemia on coronary atherosclerotic plaque progression and composition in pigs. *Int J Cardiol*. 2013;169:394–401. doi: 10.1016/j.ijcard.2013.10.021.
2. Koskinas KC, Sukhova GK, Baker AB, Papafaklis MI, Chatzizisis YS, Coskun AU, Quillard T, Jonas M, Maynard C, Antoniadis AP, Shi GP, Libby P, Edelman ER, Feldman CL, Stone PH. Thin-capped atheromata with reduced collagen content in pigs develop in coronary arterial regions exposed to persistently low endothelial shear stress. *Arterioscler Thromb Vasc Biol*. 2013;33:1494–1504. doi: 10.1161/ATVBAHA.112.300827.
3. Phinikaridou A, Hua N, Pham T, Hamilton JA. Regions of low endothelial shear stress colocalize with positive vascular remodeling and atherosclerotic plaque disruption: an in vivo magnetic resonance imaging study. *Circ Cardiovasc Imaging*. 2013;6:302–310. doi: 10.1161/CIRCIMAGING.112.000176.
4. Chatzizisis YS, Baker AB, Sukhova GK, Koskinas KC, Papafaklis MI, Beigel R, Jonas M, Coskun AU, Stone BV, Maynard C, Shi GP, Libby P, Feldman CL, Edelman ER, Stone PH. Augmented expression and activity of extracellular matrix-degrading enzymes in regions of low endothelial shear stress colocalize with coronary atheromata with thin fibrous caps in pigs. *Circulation*. 2011;123:621–630. doi: 10.1161/CIRCULATIONAHA.110.970038.
5. Koskinas KC, Feldman CL, Chatzizisis YS, Coskun AU, Jonas M, Maynard C, Baker AB, Papafaklis MI, Edelman ER, Stone PH. Natural history of experimental coronary atherosclerosis and vascular remodeling in relation to endothelial shear stress: a serial, in vivo intravascular ultrasound study. *Circulation*. 2010;121:2092–2101. doi: 10.1161/CIRCULATIONAHA.109.901678.
6. Chatzizisis YS, Jonas M, Coskun AU, Beigel R, Stone BV, Maynard C, Gerrity RG, Daley W, Rogers C, Edelman ER, Feldman CL, Stone PH. Prediction of the localization of high-risk coronary atherosclerotic plaques on the basis of low endothelial shear stress: an intravascular ultrasound and histopathology natural history study. *Circulation*. 2008;117:993–1002. doi: 10.1161/CIRCULATIONAHA.107.695254.
7. Cheng C, Tempel D, van Haperen R, van der Baan A, Grosveld F, Daemen MJ, Krams R, de Crom R. Atherosclerotic lesion size and vulnerability are determined by patterns of fluid shear stress. *Circulation*. 2006;113:2744–2753. doi: 10.1161/CIRCULATIONAHA.105.590018.
8. Samady H, Eshtehardi P, McDaniel MC, Suo J, Dhawan SS, Maynard C, Timmins LH, Quyyumi AA, Giddens DP. Coronary artery wall shear stress is associated with progression and transformation of atherosclerotic plaque and arterial remodeling in patients with coronary artery disease. *Circulation*. 2011;124:779–788. doi: 10.1161/CIRCULATIONAHA.111.021824.
9. Stone PH, Coskun AU, Kinlay S, Popma JJ, Sonka M, Wahle A, Yeghiazarians Y, Maynard C, Kuntz RE, Feldman CL. Regions of low endothelial shear stress are the sites where coronary plaque progresses and vascular remodelling occurs in humans: an in vivo serial study. *Eur Heart J*. 2007;28:705–710. doi: 10.1093/eurheartj/ehl575.
10. Stone PH, Saito S, Takahashi S, Makita Y, Nakamura S, Kawasaki T, Takahashi A, Katsuki T, Nakamura S, Namiki A, Hirohata A, Matsumura T, Yamazaki S, Yokoi H, Tanaka S, Otsuji S, Yoshimachi F, Honye J, Harwood D, Reitman M, Coskun AU, Papafaklis MI, Feldman CL; PREDICTION Investigators. Prediction of progression of coronary artery disease and clinical outcomes using vascular profiling of endothelial shear stress and arterial plaque characteristics: the PREDICTION Study. *Circulation*. 2012;126:172–181. doi: 10.1161/CIRCULATIONAHA.112.096438.
11. Vergallo R, Papafaklis MI, Yonetsu T, Bourantas CV, Andreou I, Wang Z, Fujimoto JG, McNulty I, Lee H, Biasucci LM, Crea F, Feldman CL, Michalis LK, Stone PH, Jang IK. Endothelial shear stress and coronary plaque characteristics in humans: combined frequency-domain optical coherence tomography and computational fluid dynamics study. *Circ Cardiovasc Imaging*. 2014;7:905–911. doi: 10.1161/CIRCIMAGING.114.001932.
12. Kato K, Yonetsu T, Kim SJ, Xing L, Lee H, McNulty I, Yeh RW, Sakhuja R, Zhang S, Uemura S, Yu B, Mizuno K, Jang IK. Nonculprit plaques in patients with acute coronary syndromes have more vulnerable features compared with those with non-acute coronary syndromes: a 3-vessel optical coherence tomography study. *Circ Cardiovasc Imaging*. 2012;5:433–440. doi: 10.1161/CIRCIMAGING.112.973701.
13. Papafaklis MI, Bourantas CV, Yonetsu T, Vergallo R, Kotsia A, Nakatani S, Lakkas LS, Athanasiou LS, Naka KK, Fotiadis DI, Feldman CL, Stone PH, Serruys PW, Jang IK, Michalis LK. Anatomically correct three-dimensional coronary artery reconstruction using frequency domain optical coherence tomographic and angiographic data: head-to-head comparison with intravascular ultrasound for endothelial shear stress assessment in humans. *EuroIntervention*. 2015;11:407–415. doi: 10.4244/EIJY14M06_11.
14. Toutouzas K, Chatzizisis YS, Riga M, Giannopoulos A, Antoniadis AP, Tu S, Fujino Y, Mitsouras D, Doulaverakis C, Tsampoulatidis I, Koutkias VG, Bouki K, Li Y, Chouvarda I, Cheimariotis G, Maglaveras N, Kompatsiaris I, Nakamura S, Reiber JH, Rybicki F, Karvounis H, Stefanadis C, Tousoulis D, Giannoglou GD. Accurate and reproducible reconstruction of coronary arteries and endothelial shear stress calculation using 3D OCT: comparative study to 3D IVUS and 3D QCA. *Atherosclerosis*. 2015;240:510–519. doi: 10.1016/j.atherosclerosis.2015.04.011.
15. Jang IK, Tearney GJ, MacNeill B, Takano M, Moselewski F, Iftima N, Shishkov M, Houser S, Aretz HT, Halpern EF, Bouma BE. In vivo characterization of coronary atherosclerotic plaque by use of optical coherence tomography. *Circulation*. 2005;111:1551–1555. doi: 10.1161/01.CIR.0000159354.43778.69.
16. Prati F, Guagliumi G, Mintz GS, Costa M, Regar E, Akasaka T, Barlis P, Tearney GJ, Jang IK, Arbustini E, Bezerra HG, Ozaki Y, Bruining N, Dudek D, Radu M, Erglis A, Motreff P, Alfonso F, Toutouzas K, Gonzalo N, Tamburino C, Adriaenssens T, Pinto F, Serruys PW, Di Mario C; Expert's OCT Review Document. Expert review document part 2: methodology, terminology and clinical applications of optical coherence tomography for the assessment of interventional procedures. *Eur Heart J*. 2012;33:2513–2520. doi: 10.1093/eurheartj/ehs095.
17. Tearney GJ, Regar E, Akasaka T, Adriaenssens T, Barlis P, Bezerra HG, Bouma B, Bruining N, Cho JM, Chowdhary S, Costa MA, de Silva R, Dijkstra J, Di Mario C, Dudek D, Dudeck D, Falk E, Falk E, Feldman MD, Fitzgerald P, Garcia-Garcia HM, Garcia H, Gonzalo N, Granada JF, Guagliumi G, Holm NR, Honda Y, Ikeno F, Kawasaki M, Kochman J, Koltowski L, Kubo T, Kume T, Kyono H, Lam CC, Lamouche G, Lee DP, Leon MB, Maehara A, Manfrini O, Mintz GS, Mizuno K, Morel MA, Nadkarni S, Okura H, Otake H, Pietrasik A, Prati F, Räber L, Radu MD, Rieber J, Riga M, Rollins A, Rosenberg M, Sirbu V, Serruys PW, Shimada K, Shinke T, Shite J, Siegel E, Sonoda S, Sonada S, Suter M, Takarada S, Tanaka A, Terashima M, Thim T, Troels T, Uemura S, Ughi GJ, van Beusekom HM, van der Steen AF, van Es GA, van Es GA, van Soest G, Virmani R, Waxman S, Weissman NJ, Weisz G; International Working Group for Intravascular Optical Coherence Tomography (IWG-IVOCT). Consensus standards for acquisition, measurement, and reporting of intravascular optical coherence tomography studies: a report from the International Working Group for Intravascular Optical Coherence Tomography Standardization and Validation. *J Am Coll Cardiol*. 2012;59:1058–1072. doi: 10.1016/j.jacc.2011.09.079.
18. Qi YX, Qu MJ, Long DK, Liu B, Yao QP, Chien S, Jiang ZL. Rho-GDP dissociation inhibitor alpha downregulated by low shear stress promotes vascular smooth muscle cell migration and apoptosis: a proteomic analysis. *Cardiovasc Res*. 2008;80:114–122. doi: 10.1093/cvr/cvn158.
19. Tricot O, Mallat Z, Heymes C, Belmin J, Lesèche G, Tedgui A. Relation between endothelial cell apoptosis and blood flow direction in human atherosclerotic plaques. *Circulation*. 2000;101:2450–2453.
20. Stone PH, Coskun AU, Kinlay S, Clark ME, Sonka M, Wahle A, Ilegbusi OJ, Yeghiazarians Y, Popma JJ, Orav J, Kuntz RE, Feldman CL. Effect of endothelial shear stress on the progression of coronary artery disease, vascular remodeling, and in-stent restenosis in humans: in vivo 6-month follow-up study. *Circulation*. 2003;108:438–444. doi: 10.1161/01.CIR.0000080882.35274.AD.
21. Virmani R, Kolodgie FD, Burke AP, Farb A, Schwartz SM. Lessons from sudden coronary death: a comprehensive morphological classification scheme for atherosclerotic lesions. *Arterioscler Thromb Vasc Biol*. 2000;20:1262–1275.
22. Burke AP, Kolodgie FD, Farb A, Weber D, Virmani R. Morphological predictors of arterial remodeling in coronary atherosclerosis. *Circulation*. 2002;105:297–303.

23. Korshunov VA, Berk BC. Strain-dependent vascular remodeling: the "Glagov phenomenon" is genetically determined. *Circulation*. 2004;110:220–226. doi: 10.1161/01.CIR.0000134958.88379.2E.
24. Chatzizisis YS, Coskun AU, Jonas M, Edelman ER, Feldman CL, Stone PH. Role of endothelial shear stress in the natural history of coronary atherosclerosis and vascular remodeling: molecular, cellular, and vascular behavior. *J Am Coll Cardiol*. 2007;49:2379–2393. doi: 10.1016/j.jacc.2007.02.059.
25. Di Vito L, Imola F, Gatto L, Romagnoli E, Limbruno U, Marco V, Picchi A, Micari A, Albertucci M, Prati F. Limitations of OCT in identifying and quantifying lipid components: an in vivo comparison study with IVUS-NIRS. *EuroIntervention*. 2017;13:303–311. doi: 10.4244/EIJ-D-16-00317.

Low Endothelial Shear Stress Predicts Evolution to High-Risk Coronary Plaque Phenotype in the Future: A Serial Optical Coherence Tomography and Computational Fluid Dynamics Study

Erika Yamamoto, Gerasimos Siasos, Marina Zaromytidou, Ahmet U. Coskun, Lei Xing, Krzysztof Bryniarski, Thomas Zanchin, Tomoyo Sugiyama, Hang Lee, Peter H. Stone and Ik-Kyung Jang

Circ Cardiovasc Interv. 2017;10:
doi: 10.1161/CIRCINTERVENTIONS.117.005455
Circulation: Cardiovascular Interventions is published by the American Heart Association, 7272 Greenville Avenue, Dallas, TX 75231

Print ISSN: 1941-7640. Online ISSN: 1941-7632

Supplemental material

Supplemental methods

Three-dimensional coronary artery reconstruction

Three-dimensional coronary artery reconstruction was performed using coronary angiograms and FD-OCT images. Two images were selected from the angiographic projections that portrayed the most distal and proximal anatomic landmarks detected also in the FD-OCT images. The portion of the artery defined from the distal and proximal anatomic landmarks was reconstructed using the FD-OCT data. FD-OCT image sequences were reviewed to identify the most common distal and proximal fiduciary marks (i.e., side branches) that were visible in both FD-OCT and coronary angiograms. The reconstruction methodology used the 3D luminal centerline derived from the angiographic projections as a backbone to reconstruct the coronary artery, thereby incorporating the 3D curved course of the artery with any local curvature on the epicardial surface into the 3D coronary model.[1] The borders of the lumen were detected in the FD-OCT images. The selected end-diastolic angiograms were processed for edge detection of the lumen borders and then estimation of the luminal centerline.[1] The 2 centerlines assessed in the angiograms were used to define 2 B-splines which were extruded normal to their plane, each one forming a surface.[1] The intersection of the 2 surfaces was a 3D curve, which corresponded to the 3D luminal centerline. The center of the lumen area from the

FD-OCT images was determined and the OCT-derived lumen borders were placed perpendicularly onto the 3D lumen centerline in equidistant locations, matching center of lumen in the OCT image to the 3D centerline. The relative rotational orientation of the FD-OCT frames was estimated using 3D geometry algorithms, whereas the absolute rotational orientation of the first FD-OCT frame was estimated using the orientation of side branches. The lumen 3D boundary points derived from the abovementioned methodology were connected to build the FD-OCT–based lumen geometry in 3D space.

Blood Flow simulation and ESS calculation

The obtained 3D coronary geometry, reconstructions were further processed with CFD techniques, which can provide detailed characteristics of intravascular blood flow and local ESS distribution. These techniques involve the generation of a finite volume mesh to perform blood flow simulation by solving the 3D transport equations governing the conservation of mass and momentum (PHOENICS, CHAM, London, UK).[2] Coronary blood flow for the reconstructed arterial segment was calculated directly from the time required for the volume of blood contained within the segment to be displaced by radio-opaque material during a contrast injection. The true 3D volume of the segment was first computed from the 3D lumen reconstruction. The number of cine-frames required for the contrast medium to pass from the inlet to the outlet of the studied segment was calculated. The flow rate (mL/s)

was calculated as (frame rate [frames/sec]×volume [mL])/frame count.[1] Blood rheological behavior was approximated by a homogeneous and Newtonian fluid with a viscosity estimated from Hematocrit and average shear rate in the artery and a density of 1050 kg/m.[2-5] Blood flow was considered to be laminar and incompressible and the no-slip condition assuming rigid walls was applied. ESS at the endothelial surface of the artery was calculated as the product of blood viscosity and the gradient of blood velocity at the wall.

Supplemental Reference

1. Papafaklis MI, Bourantas CV, Yonetsu T, Vergallo R, Kotsia A, Nakatani S, Lakkas LS, Athanasiou LS, Naka KK, Fotiadis DI, Feldman CL, Stone PH, Serruys PW, Jang IK, Michalis LK. Anatomically correct three-dimensional coronary artery reconstruction using frequency domain optical coherence tomographic and angiographic data : head-to-head comparison with intravascular ultrasound for endothelial shear stress assessment in humans. *EuroIntervention*. 2015;11:407–415. doi: 10.4244/EIJY14M06_11

2. Papafaklis MI, Bourantas CV, Theodorakis PE, Katsouras CS, Fotiadis DI, Michalis LK. Relationship of shear stress with in-stent restenosis: Bare metal stenting and the effect of brachytherapy. *Int J Cardiol*. 2009;134:25–32. doi: 10.1016/j.ijcard.2008.02.006

3. Wentzel JJ, Krams R, Schuurbiers JC, Oomen JA, Kloet J, van Der Giessen WJ, Serruys PW, Slager CJ. Relationship between neointimal thickness and shear stress after Wallstent implantation in human coronary arteries. *Circulation*. 2001;103:1740–1745.

4. Rikhtegar F, Knight JA, Olgac U, Saur SC, Poulikakos D, Marshall W, Cattin PC, Alkadhi H, Kurtcuoglu V. Choosing the optimal wall shear parameter for the prediction of plaque location-A patient-specific computational study in human left coronary arteries. *Atherosclerosis*. 2012;221:432–437. doi: 10.1016/j.atherosclerosis.2012.01.018

5. Coskun AU, Yeghiazarians Y, Kinlay S, Clark ME, Ilegbusi OJ, Wahle A, Sonka M, Popma JJ, Kuntz RE, Feldman CL, Stone PH. Reproducibility of coronary lumen, plaque, and vessel wall reconstruction and of endothelial shear stress measurements in vivo in humans. *Catheter Cardiovasc Interv*. 2003;60:67–78. doi: 10.1002/ccd.10594